

## PAPER

[View Article Online](#)  
[View Journal](#) | [View Issue](#)

Cite this: *Dalton Trans.*, 2025, **54**, 1929

Received 11th November 2024,  
Accepted 11th December 2024

DOI: 10.1039/d4dt03155e

rsc.li/dalton

# A zirconocene triazenido hydride complex activates CO<sub>2</sub>†

Charlotte Proges,<sup>a</sup> Kevin Lindenau,<sup>a</sup> Julia Rothe,<sup>a,b</sup> Anke Spannenberg,<sup>a</sup> Wolfgang Baumann,<sup>a</sup> Fabian Reiß,<sup>a</sup> Axel Schulz<sup>a,b</sup> and Torsten Beweries<sup>a\*</sup>

Starting from the alkyne complex Cp<sub>2</sub>Zr(py)(η<sup>2</sup>-Me<sub>3</sub>SiC<sub>2</sub>SiMe<sub>3</sub>) (Cp = η<sup>5</sup>-cyclopentadienyl, py = pyridine), the synthesis and complete characterisation of a zirconocene(IV) triazenido hydride complex and its use in the activation of small molecules is reported. The reaction with CO<sub>2</sub> led to the formation of a zirconocene(IV) triazenido-formate complex, which was further investigated for its stability towards different bases with respect to the formation of formic acid. The experimentally observed reaction pathway was investigated computationally using DFT methods, revealing the favourable role of pyridine coordination in the hydrogen transfer from the triazene to the alkyne unit of the zirconocene reagent.

## Introduction

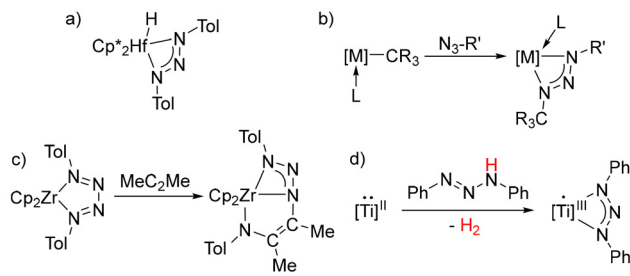
In coordination chemistry, bidentate anionic bases with nitrogen donor sites such as amidinates, guanidates and β-diketiminates play a crucial role in stabilising and shielding reactive sites, making them widely used and extensively studied ligands.<sup>1</sup> Interestingly, structurally related triazenido ligands have received comparatively less attention. Due to their two- or four-electron donor character, triazenido ligands exhibit a wide range of structural chemistry. They can either coordinate in monodentate<sup>2</sup> or bidentate<sup>3</sup> mode to a single metal fragment and serve as bridging ligands between two metal centres.<sup>3a,4</sup>

In group 4 coordination chemistry, several documented routes have been established for the introduction of these types of ligands. One of the first reported examples is the use of 1,3-tolyltriazene and hafnocene hydrides, which forms a triazenido hydride complex (Fig. 1a).<sup>5</sup> Furthermore, insertion of organic azides into M–C bonds allows the synthesis of unsymmetrical triazenido complexes (Fig. 1b).<sup>6</sup> A rather unusual protocol includes the insertion of alkynes into an N–N bond in zirconium tetraazadienediyl complexes (Fig. 1c).<sup>7</sup>

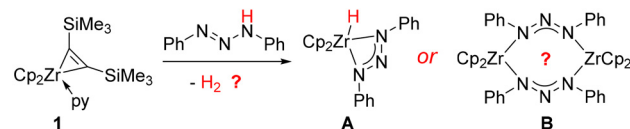
The use of free triazenes as starting materials was investigated using various sources of reactive group 4 metal frag-

ments. Both, the prior basic treatment of free triazenes<sup>8</sup> with subsequent transmetallation to the group 4 metal,<sup>9</sup> as well as direct treatment with basic group 4 metal amido complexes, form products of the type [M(RNNNR)<sub>m</sub>(X)<sub>m</sub>] (M = Ti, Zr or Hf, X = e.g. NMe<sub>2</sub>, Cl, Cp).<sup>10</sup> It was claimed that alkyl triazenido complexes can be used to form Zr and Hf monolayers by

### Group 4 metal triazenido complexes



### This work:



- mono- or dinuclear complexes  
- onward reactivity with CO<sub>2</sub>

**Fig. 1** Top: (a) Bercaw's hafnocene triazenido hydride complex; (b) generalised representation of azide insertion into the metal carbon bond. M = Zr, Hf; R and L = various substituents; (c) synthesis of zirconocene triazenido complexes using zirconocene tetraazadienediyl complexes as starting material; (d) formation of Ti(III) triazenido complexes under release of hydrogen, starting from Ti(II) sources. Bottom: reaction of Zr(II) precursor **1**, formation of four- vs. eight-membered metallacycles.

<sup>a</sup>Leibniz Institute for Catalysis, Albert-Einstein-Str. 29a, 18059 Rostock, Germany.

E-mail: fabian.reiss@catalysis.de, torsten.beweries@catalysis.de

<sup>b</sup>Institute of Chemistry, University of Rostock, Albert-Einstein-Str. 3a, 18059 Rostock, Germany

† Electronic supplementary information (ESI) available: Experimental, spectroscopic, crystallographic, and computational details. CCDC 2342475 and 2342476. For ESI and crystallographic data in CIF or other electronic format see DOI: <https://doi.org/10.1039/d4dt03155e>

CVD,<sup>10c</sup> whereas aryl-substituted analogues can serve as pre-catalysts for olefin polymerisation.<sup>10d</sup> The use of aryl triazene and Ti(II) sources or Ti(IV) precursors has also been investigated by the Beckhaus group and by us before. Beckhaus' Ti(IV) bis(pentafulvene) complexes, formally Brønsted basic, lead to Ti(IV) triazenido complexes where the proton is transferred to one of the pentafulvene units.<sup>11</sup> Conversely Ti(II) sources such the alkyne complex  $[\text{Cp}_2\text{Ti}(\eta^2\text{-Me}_3\text{SiC}_2\text{SiMe}_3)]$  (Cp =  $\eta^5$ -cyclopentadienyl) lead to rare Ti(III) triazenido complexes under evolution of hydrogen (Fig. 1d).<sup>9,11</sup>

Considering the divergent coordination behaviour that can be observed with the related triatomic allenediide ligand  $[\text{Me}_3\text{SiCCCSiMe}_3]^{2-}$ , giving either four-membered 1-metallacyclobuta-2,3-dienes (similar to structure **A** Fig. 1 bottom) when using *ansa*-metallocenes,<sup>12</sup> or dinuclear dizirconacyclooctatetraenes with smaller metallocenes (like structure **B** Fig. 1 bottom),<sup>13,12b</sup> the question arises whether similar, hitherto unknown triazenido-bridged dinuclear zirconocene complex **B** can be prepared using Rosenthal's reagent  $[\text{Cp}_2\text{Zr}(\text{py})(\eta^2\text{-Me}_3\text{SiC}_2\text{SiMe}_3)]$  (**1**, py = pyridine) as the Zr(II) precursor<sup>14</sup> (Fig. 1, bottom). Herein we present an investigation of this reactivity and the study of the obtained first zirconocene triazenido hydride complex towards  $\text{CO}_2$ .

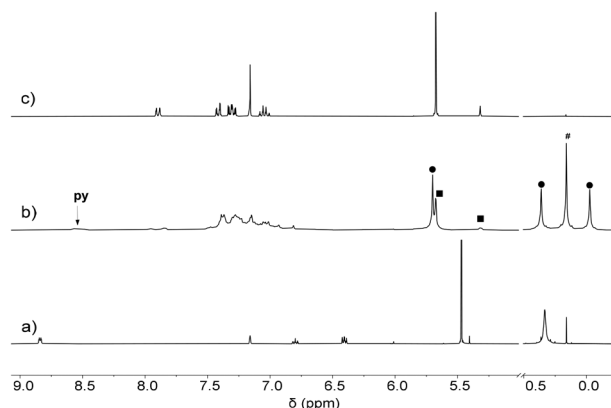
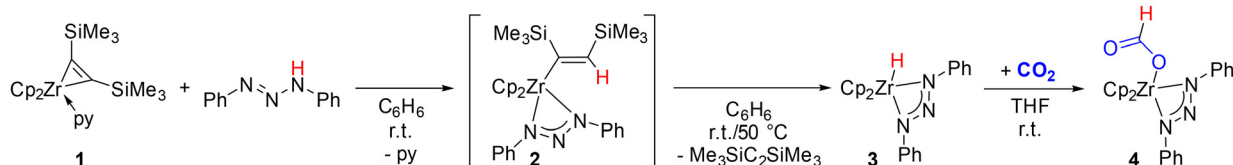


Fig. 2  $^1\text{H}$  NMR spectra of (a) complex **1** (room temperature, 300 MHz,  $\text{C}_6\text{D}_6$ ); (b) reaction mixture of **1** and 1,3-diphenyltriazene after 24 h (room temperature, 80 MHz,  $\text{C}_6\text{D}_6$ ). Labelling scheme: ●: Cp,  $\text{Me}_3\text{Si}$  of **2**; ■: Cp, Zr–H of **3**; py: free pyridine; #: free  $\text{Me}_3\text{SiCCSiMe}_3$ . (c) isolated complex **3** (room temperature, 300 MHz,  $\text{C}_6\text{D}_6$ ).

## Results and discussion

The reaction of complex **1** with an excess of 1,3-diphenyltriazene ( $\text{PhNNH}(\text{H})\text{Ph}$ ) was investigated by low-field  $^1\text{H}$  NMR spectroscopy (room temperature, 80 MHz,  $\text{C}_6\text{D}_6$ ). No evidence for  $\text{H}_2$  formation was found, corroborated by the absence of the characteristic resonance at  $\delta$  4.47 ppm.<sup>15</sup> However, the  $^1\text{H}$  NMR spectra show the full consumption of **1** (Fig. 2a and b), as well as two new prominent resonances in the  $\text{SiMe}_3$  region (Fig. 2b,  $\delta$  0.36,  $-0.03$  ppm) and a characteristic signal for Cp protons ( $\delta$  5.70 ppm). Furthermore, an isolated resonance of free pyridine ( $\delta$  8.53 ppm,  $\text{CH-2,6}$ )<sup>15</sup> indicates ligand exchange in the first step, likely forming the complex  $[\text{Cp}_2\text{Zr}(\text{PhNNHPh})\text{Me}_3\text{SiC}(\text{H})\text{CSiMe}_3]$  (**2**, Scheme 1). Monitoring the prominent  $\text{SiMe}_3$  signals for 75 hours at room temperature suggests that **2** is a transient species. During this time the signal of non-coordinated  $\text{Me}_3\text{SiC}_2\text{SiMe}_3$  ( $\delta$  0.16 ppm) increases with decreasing reaction rate, which allows a first-order follow-up reaction to be estimated (Fig. S1 and S2†). Although full conversion is not achieved after 80 h at room temperature, slow formation of a new zirconocene species occurs with characteristic resonances for Cp protons ( $\delta$  5.68 ppm) and an additional broad N–H or Zr–H signal at  $\delta$  5.30 ppm. To support the proposed structure of **2** a series of *in situ* 2D-NMR experiments were performed at ambient temperature and at  $T = -20^\circ\text{C}$  which agree with the proposed zirconocene triazenido vinyl complex structure (Fig. S4–S11†). Formation of complex **2** probably occurs by exchange of the pyridine for the triazene ligand and subsequent transfer of the triazenido NH proton to the alkyne ligand, corroborated by its characteristic  $^1\text{H}$  ( $\delta$  6.76 ppm) and  $^{29}\text{Si}$  ( $\delta$   $-9.7$  ppm,  $J_{\text{SiH}} = 23$  Hz) resonances (Fig. S8–S11†). Ligand substitution is a common process in zirconocene chemistry and is also used in the synthesis of **1**, where THF is replaced by a pyridine ligand.<sup>16</sup>

Proton transfer reactions, in particular from acidic groups to the alkyne  $\text{Me}_3\text{SiC}_2\text{SiMe}_3$ , are well known.<sup>17</sup> However, reactions in which the hydrogen atom of the resulting alkenyl/vinyl group undergoes a subsequent shift along with elimination of the alkyne, are much rarer.<sup>18</sup> The reactivity described here is reminiscent of that of the chemically related *N,N'*-diphenylformamidine with **1**, in which a complex similar to **2** was identified. Upon heating this species formed the Zr hydrido complex  $[\text{Cp}_2\text{Zr}(\text{H})\text{PhNC}(\text{H})\text{NPh}]$ , suggesting the formation of an analogous complex in our case.<sup>18b</sup> With this in mind, we then focused on the more stable follow-up reaction product identified in our NMR monitoring experiments. To bypass the long



Scheme 1 Summary of the reaction sequence of the Rosenthal complex **1** with diphenyltriazene at room temperature, giving spectroscopically characterised intermediate **2** and the zirconocene hydride complex **3**. Selective formation of **3** at  $T = 50^\circ\text{C}$ , onward reactivity with  $\text{CO}_2$  and formation of **4**.



reaction time observed, a 1 : 1 mixture of **1** and 1,3-diphenyltriazene was reacted in C<sub>6</sub>H<sub>6</sub> for 18 hours at 50 °C, giving a clear dark red solution. Single crystals suitable for single crystal X-ray diffraction (SC-XRD) analysis of the follow-up product **3** (Fig. 3, left) could be obtained after addition of pentane to the concentrated reaction solution at −78 °C. The molecular structure reveals the formation of a zirconocene triazenido hydrido species, similar to Bercaw's hafnocene hydrido complex (Fig. 1a), which explains the lack of hydrogen evolution and again shows the preferential chelating coordination of the NNN unit. A comparison of <sup>1</sup>H NMR resonances of redissolved (C<sub>6</sub>D<sub>6</sub>) isolated crystals of **3** and those observed in the above monitoring experiment (Fig. 2b and c) shows excellent agreement. Due to the moderate solubility of **3** in C<sub>6</sub>D<sub>6</sub>, further NMR analysis was performed in THF-*d*<sub>8</sub>, where the Cp signal shifts to δ 6.05 ppm and the Zr–H resonates at δ 5.17 ppm. The presence of a hydride in **3** is substantiated by the <sup>1</sup>H–<sup>15</sup>N HMBC correlation between the Zr–H signal and the terminal α-nitrogen atoms (δ −122.5/−109.6 ppm) as well as a minor correlation with the central β-nitrogen atom at δ 126.6 ppm (Fig. S15†). The large relative shift between α- and β-nitrogen signals of Δδ = 249 and 236 ppm reflects their contrasting electronic situations, ruling out a partial Zr–N<sub>β</sub> interaction (see ESI section 2.5†). The ATR-IR spectrum of **3** shows a strong ν<sub>as</sub>(NNN) vibration at 1271 cm<sup>−1</sup> and ν(Zr–H) stretching mode at 1591 cm<sup>−1</sup> in good agreement with Bercaw's heavier hafnocene congener (Fig. 1a) (ν<sub>as</sub>(NNN) = 1301, ν(Hf–H) = 1630 cm<sup>−1</sup>).<sup>19</sup>

In an initial attempt to crystallise complex **3**, a colour change of the solution from orange to yellow was observed after storing the flask in a Dewar barrel cooled with dry ice. Surprisingly, <sup>1</sup>H NMR analysis of this solution showed a different set of characteristic signals in THF-*d*<sub>8</sub> for Cp ligands (δ 6.38 ppm) and a further singlet at δ 8.28 ppm. The latter shows <sup>13</sup>C satellites with a remarkably large coupling constant (<sup>1</sup>J<sub>C,H</sub> = 205 Hz). After clarifying the formation of **3**, we focused

on this secondary finding as we had reason to assume that CO<sub>2</sub> accidentally entered the flask, resulting in serendipitous, yet selective follow-up reaction of complex **3** with the former. Reproducing this transformation by treatment of isolated crystals of **3** with CO<sub>2</sub> in THF shows a colour change of the solution from orange to yellow (Scheme 1). The <sup>1</sup>H NMR spectrum of the yellow solid obtained after workup was identical to that observed earlier, thus confirming our assumption. The <sup>1</sup>H–<sup>15</sup>N HMBC spectrum neither shows correlation between the new resonance at δ 8.28 ppm and the α-nitrogen atoms (−113.3/−97.7 ppm) nor with the β-nitrogen atom (Fig. S20†),<sup>20</sup> indicating CO<sub>2</sub> insertion into the Zr–H bond. This assumption could be confirmed by SC-XRD analysis, which revealed the formation of a zirconocene triazenido formate complex **4** (Fig. 3, right). Based on this finding, the new <sup>1</sup>H NMR resonance at low field can be assigned to the formate ligand. The insertion of CO<sub>2</sub> into metal hydride bonds is a well-documented reaction, particularly in late transition metal chemistry, where the catalytic reduction of CO<sub>2</sub> with hydrogen to formic acid has been studied in detail.<sup>21</sup> Of note, there are comparably few examples of such insertion reactions in group 4 metal chemistry. These studies were carried out in the context of frustrated Lewis pair chemistry, showing the same behaviour.<sup>22</sup> To our knowledge, only one comparable isolated zirconocene formate complex was reported before, showing a formate <sup>1</sup>H NMR resonance at δ 8.87 ppm (C<sub>6</sub>D<sub>6</sub>) that agrees well with the value of **4**.<sup>22a</sup> Formation of such species was observed as an intermediate in the reaction of the related Schwartz reagent Cp<sub>2</sub>Zr(H)Cl with CO<sub>2</sub> which furnishes formaldehyde and the dinuclear complex μ-O-[Cp<sub>2</sub>ZrCl]<sub>2</sub>.<sup>23</sup> This onward reactivity contrasts with the herein reported formation of a stable, mononuclear formate complex **4**, likely due to the presence of the sterically demanding triazene ligand. In previous studies, hydrogenation of the formate with bulky Lewis acids as a further activating agent was attempted, however, formation of formic acid was not found.

To deepen our understanding of the observed reactivity, a two-step computational analysis was carried out. First, the observed reaction pathway and its possible transition states were investigated using the semi-empirical GFN2-xTB method,<sup>24</sup> followed by a DFT re-optimisation and verification at the B3LYP<sup>25</sup>-D3<sup>26</sup>/def2-TZVP<sup>27</sup> level. The rapid formation of **2** from **1** suggests that in the first step the pyridine ligand is exchanged by the coordination of one nitrogen of the triazene unit. To our surprise, the subsequent hydrogen transfer from the triazene NH to the alkyne unit in this structure shows an activation barrier of ΔG<sup>‡</sup> = 138.5 kJ mol<sup>−1</sup>, which is not compatible with the experimentally observed fast formation of **2** under ambient conditions. Therefore, the influence of the pyridine ligand on this transformation was further evaluated and coordination of the 1,3-diphenyltriazene unit in between the pyridine and alkyne ligand was found to be preferred (Fig. 4, **Int1**). Starting from this structure, four different reaction pathways were explored at the GFN2-xTB level of theory (Fig. S37†), revealing that a hydrogen shift to the pyridine and pyridine decoordination is rather unlikely. Interestingly, the hydrogen shift to the alkyne unit shows the lowest estimated energy

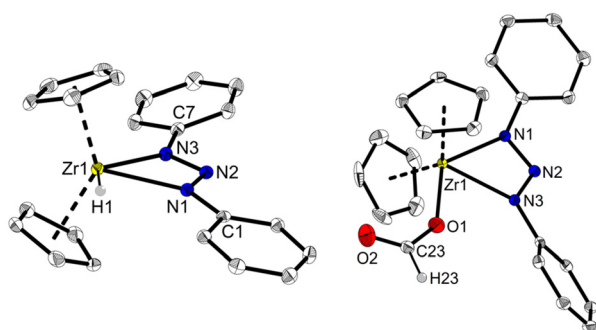


**Fig. 3** Molecular structures of complexes **3** (left) and **4** (right). Thermal ellipsoids correspond to 30% probability (**3**: 110 K; **4**: 150 K). Hydrogen atoms except H1 in **3** and H23 in **4** as well as the second molecule of **3** from the asymmetric unit are omitted for clarity. Selected bond lengths for **3**: Zr1–N1 2.336(2); Zr1–N3 2.332(2); N1–N2 1.314(3); N2–N3 1.312(3); second molecule: Zr2–N4 2.333(2), Zr2–N6 2.337(2), N4–N5 1.308(3), N5–N6 1.306(3). **4**: Zr1–N1 2.360(2); Zr1–N3 2.300(2); N1–N2 1.304(2); N2–N3 1.314(2).



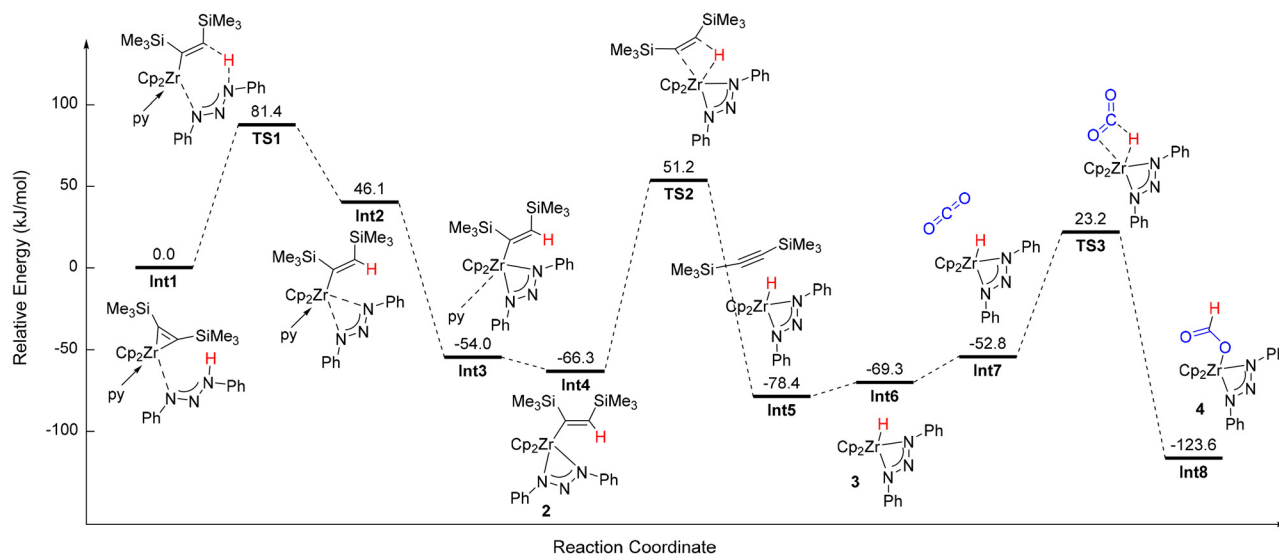


Fig. 4 Calculated relative Gibbs free reaction energies along the experimentally observed reaction sequence based on experimentally identified complexes 2–4. Level of theory B3LYP-D3/def2-TZVP/uncorrected in gas phase.

barrier and the second highest energy gain, which agrees with the experiment and therefore this pathway was investigated further on a higher level of theory. The consideration of pyridine in **Int1** leads to a remarkable decrease of the activation barrier for the hydrogen shift (**TS1**,  $\Delta G^\ddagger = 81.4 \text{ kJ mol}^{-1}$ ) followed by strongly favoured pyridine de-coordination *via* **Int2** and **Int3** leading to complex **2** (Fig. 4, **Int4**,  $\Delta_R G^\theta = -66.3 \text{ kJ mol}^{-1}$ ). It was not possible to locate a transition state structure between **Int2** and **Int3** probably due to the flat energy surface connecting these species. The subsequent hydrogen shift from the vinyl group of **2** to the Zr centre in **3** (**Int6**), shows the highest-lying transition state of the entire reaction sequence (**TS2**,  $\Delta G^\ddagger = 117.6 \text{ kJ mol}^{-1}$ ), which explains the rather slow reaction at ambient temperature or the need for thermal activation. The rapid formation of highly exergonic complex **4** (**Int8**,  $\Delta_R G^\theta = -123.6 \text{ kJ mol}^{-1}$ ) at ambient conditions is well explained by the low-lying transition state (**TS3**,  $\Delta G^\ddagger = 76.0 \text{ kJ mol}^{-1}$ ). Although transition states could not be localised for all reaction steps, in particular for substrate coordination and de-coordination, presumably due to flat potential energy surfaces, the calculations show very good agreement with the observed experimental behaviour and shed light on a likely reaction pathway. Particularly noteworthy are the lowered activation barrier for the NH shift to the alkyne unit due to additional pyridine coordination at Zr and the activation barrier of  $117.6 \text{ kJ mol}^{-1}$  for the rate-determining step of the H transfer to the Zr centre. Next, the possibility of catalytic use of complex **3** for the reduction of  $\text{CO}_2$  with  $\text{H}_2$  was studied. While the formation of **4** from **3** and  $\text{CO}_2$  is exergonic ( $\Delta_R G^\theta = -54.3 \text{ kJ mol}^{-1}$ ), the regeneration of **3** with  $\text{H}_2$  and elimination of formic acid is strongly endergonic ( $\Delta_R G^\theta = 105.8 \text{ kJ mol}^{-1}$ ) and lies at the upper limit of a reaction possible at ambient conditions (Fig. S40†). Nevertheless, this motivated us to conduct a series of NMR experiments to shed more light on

this transformation. Heating complex **4** at  $80^\circ\text{C}$  in hydrogen atmosphere did not lead to any reaction (Fig. S25†). The hydrogenation of  $\text{CO}_2$  is endergonic; however, the reaction can be influenced by the addition of a base, producing formate salts, which can lead to an exergonic reaction.<sup>28</sup> For example, Leitner and co-workers used methyldiethanolamine to facilitate the iridium-catalysed hydrogenation of  $\text{CO}_2$ .<sup>29</sup> The impact of the addition of different bases was investigated by a series of stability tests on the NMR scale (see ESI Fig. S28–33†). Complexes **3** and **4** were dissolved in  $\text{THF-}d_8$  and approx. 10 equiv. of the bases triethyl amine ( $\text{NEt}_3$ ), pyridine and 1,8-diazabicyclo(5.4.0)undec-7-ene (DBU) were added. From the resulting samples a series of  $^1\text{H}$  NMR spectra were recorded, revealing that virtually no reaction takes place when adding  $\text{NEt}_3$  or pyridine to **3** or **4**, even after a reaction time of several days at room temperature. The same was observed with **3** and DBU. However, when the Ar atmosphere was replaced by  $\text{CO}_2$  in this case, the  $^1\text{H}$  NMR spectra showed formation of unknown Cp resonances. Decomposition into an ill-defined mixture was also observed when DBU was added to independently synthesised **4**. In turn, the addition of hydrogen to samples containing **4** and pyridine or  $\text{NEt}_3$  shows practically no changes in the  $^1\text{H}$  NMR spectra. No hydrogen consumption or decrease in the signals for **4** was detected, even after three days at  $60^\circ\text{C}$  (Fig. S34 and 35†). Another possibility to facilitate the reaction of **4** back to **3** may be the addition of a hydride source. This was investigated using a 1:1 ratio of  $\text{Et}_2\text{SiH}_2$  and **4** in  $\text{THF-}d_8$ , however, the  $^1\text{H}$  NMR spectra remain unchanged at ambient conditions or after heating to  $50^\circ\text{C}$  for three days (Fig. S36†). Additionally, the stability of complexes **3** and **4** in the presence of formic acid itself was tested in  $\text{THF-}d_8$  solutions. Both complexes were not stable under these conditions with **3** reacting to **4** and molecular hydrogen and complex **4** further reacting to an unidentified species (Fig. S26





and 27†). Broadening of the excess formic acid signal could suggest an exchange of the formate ligand.

## Conclusions

In summary, the synthesis of a new zirconocene(IV) triazenido hydride complex starting from Rosenthal's reagent  $[\text{Cp}_2\text{Zr}(\text{py})(\eta^2\text{-Me}_3\text{SiC}_2\text{SiMe}_3)]$  is reported. The zirconocene(IV) hydride complex shows facile activation of  $\text{CO}_2$  to form a rare example of a Zr(IV) formate complex. A computational study of the reaction pathway reveals a lowering of the activation barrier for the first reaction step of hydrogen transfer from the diphenyltriazene to the alkyne unit when pyridine is coordinated to the zirconium centre compared to a path in which pyridine is exchanged by diphenyltriazene before this hydrogen shift. Attempts to produce formic acid through hydrogenation of the Zr(IV) formate complex were unsuccessful thus far. The reaction of the potentially catalytically active Zr hydride species with formic acid to form the formate complex was found to be a limiting factor for a catalytic reaction in a single-phase system. To avoid this, subsequent studies with two-phase systems and/or other substituents on both Cp and triazene ligands should be performed.

## Author contributions

A. S., T. B. and F. R. conceived and conceptualised the project. C. P., K. L., J. R., and F. R. performed the experiments and analysed the data. W. B. performed NMR experiments and analysed the data. A. Sp. performed SC-XRD measurement and structure refinement. F. R. performed DFT calculations and analysed the data. F. R. and T. B. supervised the project. A. S. and T. B. acquired funding. All authors discussed the data, prepared, and revised the manuscript.

## Data availability

The data, experimental description and computational details supporting this article have been included as part of the ESI† which is free of charge. In addition, the calculated optimized structures are provided in a multiple structure xyz file. Crystallographic data for 3 and 4 have been deposited at the CCDC database (3: 2342475; 4: 2342476†).

## Conflicts of interest

There are no conflicts to declare.

## Acknowledgements

We thank our technical and analytical staff for assistance. General support by LIKAT and the DFG Research Training

Group 2943 ("SPECTRE") is gratefully acknowledged. F. R. thanks the ITMZ at the University of Rostock for access to the Cluster Computer and especially M. Willert for technical support.

## References

- Selected examples: (a) F. T. Edelmann, *Chem. Soc. Rev.*, 2009, **38**, 2253; (b) F. T. Edelmann, *Chem. Soc. Rev.*, 2012, **41**, 7657; (c) L. Bourget-Merle, M. F. Lappert and J. R. Severn, *Chem. Rev.*, 2002, **102**, 3031; (d) S. P. Sarish, S. Nembenna, S. Nagendran and H. W. Roesky, *Acc. Chem. Res.*, 2011, **44**, 157; (e) Y.-C. Tsai, *Coord. Chem. Rev.*, 2012, **256**, 722; (f) D. Kalden, S. Kriek, H. Görls and M. Westerhausen, *Dalton Trans.*, 2015, **44**, 8089–8099.
- Selected examples: (a) G. Bombieri, A. Immirzi and L. Toniolo, *Inorg. Chem.*, 1976, **15**, 2428–2432; (b) A. Immirzi, G. Bombieri and L. Toniolo, *J. Organomet. Chem.*, 1976, **118**, 355–362; (c) A. Immirzi, W. Porzio, G. Bombieri and L. Toniolo, *J. Chem. Soc., Dalton Trans.*, 1980, **7**, 1098; (d) L. G. Kuz'mina, Y. T. Struchkov and D. N. Kravtsov, *J. Struct. Chem.*, 1979, **20**, 470–471.
- Selected examples of non-group 4 complexes: (a) F. A. Cotton, G. W. Rice and J. C. Sekutowski, *Inorg. Chem.*, 1979, **18**, 1143–1149; (b) M. H. Chisholm, D. A. Haitko, J. C. Huffman and K. Folting, *Inorg. Chem.*, 1981, **20**, 171–174; (c) R. Litlabø, H. S. Lee, M. Niemeyer, K. W. Törnroos and R. Anwender, *Dalton Trans.*, 2010, **39**, 6815–6825.
- (a) M. H. Chisholm, H. T. Chiu, J. C. Huffman and R. J. Wang, *Inorg. Chem.*, 1986, **25**, 1092–1096; (b) N. G. Connelly, C. J. Finn, M. J. Freeman, A. G. Orpen and J. Stirling, *J. Chem. Soc., Chem. Commun.*, 1984, **15**, 1025–1027; (c) A. L. Johnson, A. M. Willcocks and S. P. Richards, *Inorg. Chem.*, 2009, **48**, 8613–8622.
- G. L. Hillhouse and J. E. Bercaw, *Organometallics*, 1982, **1**, 1025–1029.
- (a) K. Schwitalla, W. Lee, M. Fischer, M. Schmidtman and R. Beckhaus, *Organometallics*, 2023, **42**, 1259–1266; (b) M. Manßen, I. Weimer, C. Adler, M. Fischer, M. Schmidtman and R. Beckhaus, *Eur. J. Inorg. Chem.*, 2018, 131–136; (c) S. Zhang, J. Zhao, W.-X. Zhang and Z. Xi, *Org. Lett.*, 2011, **13**, 1626–1629; (d) S. Leshinski, T. Shalumova, J. M. Tanski and R. Waterman, *Dalton Trans.*, 2010, **39**, 9073–9078; (e) T. Luker, R. J. Whitby and M. Webster, *J. Organomet. Chem.*, 1995, **492**, 53.
- K. E. Meyer, P. J. Walsh and R. G. Bergman, *J. Am. Chem. Soc.*, 1995, **117**, 974–985.
- Selected examples of group 1 and group 2 triazenide complexes: (a) M. R. Gyton, A. R. Leverett, M. L. Cole and A. I. McKay, *Dalton Trans.*, 2020, **49**, 5653–5661; (b) A. R. Leverett, V. Diachenko, M. L. Cole and A. I. McKay, *Dalton Trans.*, 2019, **48**, 13197–13204; (c) D. Kalden, S. Kriek, H. Görls and M. Westerhausen, *Dalton Trans.*, 2015, **44**, 8089–8099.



- 9 T. Beweries, F. Reiß, J. Rothe, A. Schulz and A. Villinger, *Eur. J. Inorg. Chem.*, 2019, 1993–1998.
- 10 (a) K. Soussi, S. Mishra, E. Jeanneau, A. Mantoux and S. Daniele, *Polyhedron*, 2018, **152**, 84–89; (b) I. A. Guzei, L. M. Liable-Sands, A. L. Rheingold and C. H. Winter, *Polyhedron*, 1997, **16**, 4017–4022; (c) J. Sundermeyer, S. Pulz and F. Schroeder, WO2019115646 A1, 2019; (d) V. C. Gibson, D. F. Reardon and A. K. Tomov, WO2004063233 A2, 2004.
- 11 K. Schwitalla, W. Lee, I. Töben, M. Eilers, M. Schmidtman and R. Beckhaus, *Z. Anorg. Allg. Chem.*, 2024, e202300230.
- 12 (a) F. Reiss, M. Reiss, J. Bresien, A. Spannenberg, H. Jiao, W. Baumann, P. Arndt and T. Beweries, *Chem. Sci.*, 2019, **10**, 5319–5325; (b) X. Shi, S. Li, M. Reiss, A. Spannenberg, T. Holtrichter-Rossmann, F. Reiss and T. Beweries, *Chem. Sci.*, 2021, **12**, 16074–16084; (c) X. Z. Shi, S. H. Li, A. Spannenberg, F. Reiss and T. Beweries, *Inorg. Chem. Front.*, 2023, **10**, 3584–3594; (d) S. Li, M. Schroder, A. Prudlik, X. Shi, A. Spannenberg, J. Rabeah, R. Francke, B. Corzilius, F. Reiss and T. Beweries, *Chem. – Eur. J.*, 2024, **30**, e202400708.
- 13 F. Reiß, M. Reiß, A. Spannenberg, H. Jiao, W. Baumann, P. Arndt, U. Rosenthal and T. Beweries, *Chem. – Eur. J.*, 2018, **24**, 5667–5674.
- 14 U. Rosenthal, A. Ohff, W. Baumann, A. Tillack, H. Görls, V. V. Burlakov and V. B. Shur, *Z. Anorg. Allg. Chem.*, 1995, **621**, 77–83.
- 15 G. R. Fulmer, A. J. M. Miller, N. H. Sherden, H. E. Gottlieb, A. Nudelman, B. M. Stoltz, J. E. Bercaw and K. I. Goldberg, *Organometallics*, 2010, **29**, 2176–2179.
- 16 J. R. Nitschke, S. Zürcher and T. D. Tilley, *J. Am. Chem. Soc.*, 2000, **122**, 10345–10352.
- 17 (a) U. Rosenthal, A. Ohff, M. Michalik, H. Görls, V. V. Burlakov and V. B. Shur, *Organometallics*, 1993, **12**, 5016–5019; (b) U. Rosenthal, A. Ohff, M. Michalik, H. Görls, V. V. Burlakov and V. B. Shur, *Angew. Chem.*, 1993, **105**, 1228–1230; (c) D. Thomas, N. Peulecke, V. V. Burlakov, B. Heller, W. Baumann, A. Spannenberg, R. Kempe, U. Rosenthal and R. Beckhaus, *Z. Anorg. Allg. Chem.*, 1998, **624**, 919–924; (d) M. Horacek, P. Stepnicka, J. Kubista, R. Gyepes and K. Mach, *Organometallics*, 2004, **23**, 3388–3397; (e) U. Jäger-Fiedler, P. Arndt, W. Baumann, A. Spannenberg, V. V. Burlakov and U. Rosenthal, *Eur. J. Inorg. Chem.*, 2005, 2842–2849.
- 18 (a) P. Arndt, W. Baumann, A. Spannenberg, U. Rosenthal, V. V. Burlakov and V. B. Shur, *Angew. Chem., Int. Ed.*, 2003, **42**, 1414–1418; (b) M. Haehnel, K. Schubert, L. Becker, P. Arndt, A. Spannenberg and U. Rosenthal, *Z. Anorg. Allg. Chem.*, 2014, **640**, 2532–2536.
- 19 It should be noted that the values given in the literature were recorded in Nujol mull.
- 20 No proton signal showed a clear correlation to the  $\beta$ -N atom. This supports the absence of a Zr–N interaction.
- 21 Selected review articles: (a) K. Sordakis, C. Tang, L. K. Vogt, H. Junge, P. J. Dyson, M. Beller and G. Laurenczy, *Chem. Rev.*, 2018, **118**, 372–433; (b) P. G. Jessop, F. Joó and C.-C. Tai, *Coord. Chem. Rev.*, 2004, **248**, 2425–2442.
- 22 (a) Z. Jian, G. Kehr, C. G. Daniliuc, B. Wibbeling, T. Wiegand, M. Siedow, H. Eckert, M. Bursch, S. Grimme and G. Erker, *J. Am. Chem. Soc.*, 2017, **139**, 6474–6483; (b) Y.-L. Liu, G. Kehr, C. G. Daniliuc and G. Erker, *Organometallics*, 2017, **36**, 3407–3414; (c) A. M. Chapman, M. F. Haddow and D. F. Wass, *J. Am. Chem. Soc.*, 2011, **133**, 18463–18478.
- 23 (a) G. Fachinetti, C. Floriani and S. Pucci, *J. Chem. Soc., Chem. Commun.*, 1978, 269–270; (b) S. Gambarotta, S. Strologo, C. Floriani, A. Chiesi-Villa and C. Guastini, *J. Am. Chem. Soc.*, 1985, **107**, 6278–6282; (c) M. Wang, S. Lu, M. Bei, H. Guo and Z. Jin, *J. Organomet. Chem.*, 1993, **447**, 227–231; (d) N. E. Schlörer, E. J. Cabrita and S. Berger, *Angew. Chem., Int. Ed.*, 2002, **41**, 107–109.
- 24 C. Bannwarth, S. Ehlert and S. Grimme, *J. Chem. Theory Comput.*, 2019, **15**, 1652–1671.
- 25 And references cited therein: A. D. Becke, *J. Chem. Phys.*, 1993, **98**, 5648–5652.
- 26 S. Grimme, S. Ehrlich and L. Goerigk, *J. Comput. Chem.*, 2011, **32**, 1456–1465.
- 27 F. Weigend and R. Ahlrichs, *Phys. Chem. Chem. Phys.*, 2005, **7**, 3297–3305.
- 28 P. G. Jessop, T. Ikariya and R. Noyori, *Chem. Rev.*, 1995, **95**, 259–272.
- 29 K. R. Ehmann, A. Nisters, A. J. Vorholt and W. Leitner, *ChemCatChem*, 2022, **14**, e202200892.

